Two-dimensional virial and spin-wave coefficients of spin-polarized gases (H↑, D↑, ^{3}He)

Valérie Lefevre-Seguin, Henri Guignes, and Claire Lhuillier
Laboratoire de Spectroscopie Hertzienne de l'Ecole Normale Supérieure
24 rue Lhomond, 75231 Paris Cedex 05, France
(Received 25 July 1986; revised manuscript received 29 December 1986)

We present a quantum phase-shift calculation of the two-dimensional second virial coefficient B_2^{2D} and spin-wave characteristic parameters for spin-polarized quantum gases H↑, D↑, and ^{3}He. Emphasis is put on the study of quantum exchange effects which become essential in the 1-K range and below. The dependence of B_2^{2D} upon the nuclear polarization is analyzed. The calculation of statistics-independent coefficients is extended up to 50 K. The effect of a reduced dimensionality on the second virial and spin-wave coefficients is discussed and demonstrated by a comparison between 2D and 3D results. Two-dimensional bound states of helium dimers are estimated with the best present potential of Aziz *et al.* to be $E_B(^3\text{He}\text{-}^3\text{He};\ 2D) = -0.88\times10^{-5}$ K and $E_B(^3\text{He}\text{-}^4\text{He};\ 2D) = -3.38$ mK.

I. INTRODUCTION

Spin-polarized quantum fluids such as H↑, D↑, and ^{3}He are the subject of considerable interest, both theoretical and experimental, because these systems exhibit enhanced indistinguishability when only one spin state is occupied.[1]

Such effects are well known to be present in dense degenerate phases but their analysis is then difficult because of the strong correlations due to the interatomic interaction.[2–9] It was recently pointed out that even in dilute, nondegenerate gases, particle identity has nontrivial macroscopic consequences[10,11] which affect both equilibrium properties of the gas (e.g., second virial coefficient, spin susceptibility) and transport properties. A prominent feature of the theory is the prediction that "spin waves" (oscillatory spin diffusion) should exist in spin-polarized gases. Experiments have been recently performed which demonstrate the existence of spin waves in H↑ (Refs. 12 and 13), in ^{3}He diluted in ^{4}He (Ref. 14), and in pure gaseous ^{3}He↑.[15] All the work mentioned above is related to three dimensional (3D) systems but similar effects are indeed predicted to occur in two dimensions.[16,17]

Concern with two-dimensional phases came along with the achievement of spin-polarized gases. In particular, the effect of the nuclear polarization on the static and dynamic properties of the adsorbed phases still needs to be studied thoroughly. Two-dimensional phases indeed play a crucial role in experiments on spin-polarized fluids because the presence of an adsorbed phase cannot be avoided (as long as electromagnetic trap confinement is not achieved). Relaxation of the nuclear polarization (and recombination in the case of hydrogen and deuterium) occurring in the adsorbed phases is usually minimized by means of cryogenic coatings which reduce binding energies.[18–20] But, in spite of special attention to this problem, one can never prevent the formation of an adsorbed layer at low temperatures. Whether or not this adsorbed layer can be considered as a two-dimensional phase depends on the nature of the adatom-substrate pair. Rather good for ^{3}He atoms on solid substrates (H_2, Ne) (Ref. 21) this hypothesis becomes more questionable in the case of the adsorption of H↑ on superfluid helium where one should take into account the width of the wave function perpendicular to the surface and eventually the dynamic response of the ^{4}He surface to the presence of an adatom. The first of these two problems has been already addressed in great details[17,22,23] and our own study of the two-dimensional phase of H↑ is, in this respect, more academic. We nevertheless include it here for the sake of comparison of the static and dynamic properties of H↑, D↑, and ^{3}He in two dimensions.

Section II is devoted to the study of the equation of states of submonolayers of adatoms by a virial expansion. Although B_2^{2D} has already been calculated for ^{3}He and H↑,[24,25] the quantum effects of statistics have not yet been thoroughly analyzed and the role of the nuclear polarization remains to be studied in these two-dimensional systems. This is done in Sec. II where the second-virial-coefficient formalism is presented, taking explicitly into account the dependence of B_2^{2D} on the nuclear polarization. Numerical results concerning H↑, D↑, and ^{3}He are presented and discussed with comparison to the 3D case.

Section III is devoted to the study of the two-dimensional spin-wave characteristic coefficients μ, their quality factor, and D, the spin diffusion coefficient related to the damping of these waves. As was already noted in Ref. 17 for the case of H↑, the dimensionality is shown to influence strongly the order of magnitude of these coefficients at low temperatures. Besides, our results show that any tentative scaling procedure is doomed to failure because of the extreme nonlinear sensitivity of collisions of light quantum gases to dimensionality and to the de Boer parameter. All technical details and physical comments about interaction potentials, 2D scattering phase shifts, and bound states are given in Appendices A, B, and C.

II. TWO-DIMENSIONAL SECOND VIRIAL COEFFICIENT OF H↑, D↑, AND ^{3}HE: EFFECTS OF THE NUCLEAR POLARIZATON

A. Second-virial-coefficient formalism

The virial expansion of the pressure P in two dimensions is defined by a series in powers of the density, the leading terms of which are

$$\frac{PS}{Nk_BT}=1+B_2^{2D}(T)\frac{N}{S}+\cdots , \tag{1}$$

where N is the total number of atoms of the two-dimensional gas, S is the surface offered to this system, T is the temperature, k_B is the Boltzmann constant, and $B_2^{2D}(T)$ is the 2D second virial coefficient.

The major feature of this expansion is that the second virial coefficient is entirely determined by the two-body properties of the gas so that it can be deduced from the study of a fictitious system containing only two atoms (see for instance Ref. 26 about cluster properties). The Pauli principle requires a proper symmetrization of the wave function of the two atoms with respect to the electrons and the nuclei. The case of ^{3}He is the simplest: at the low energies considered here, the two electrons of each ground-state atom can be considered, on the whole, as a nondissociable boson. As a consequence, the symmetry properties of the electronic wave function do not interfere with the symmetry requirements on the nuclei, as they will below in the case of H↑. Each of the two ^{3}He nuclei of spin $\frac{1}{2}$ behaves like a fermion. Therefore, when the nuclear spins are coupled in the antisymmetric singlet state $I=0$ of the total nuclear spin, their orbital wave function must be symmetric and conversely, when the nuclear spins are coupled in the symmetric triplet state $I=1$, their orbital wave function must be antisymmetric to satisfy the global antisymmetry required for fermions.

From this argument, it can be shown that[27]

$$B_2^{2D}(^3\mathrm{He})=\langle P_S\rangle B_2^{2D+}+\langle P_T\rangle B_2^{2D-} , \tag{2}$$

where $\langle P_S\rangle$ and $\langle P_T\rangle$ are the quantum average values of the projectors on the singlet and triplet states of the total nuclear spin. The two coefficients B_2^{2D+} or B_2^{2D-} are the second virial coefficients of spinless boson (with symmetric orbital wave functions) or spinless fermions (with antisymmetric orbital wave functions).

The case of H↑ is easily analyzed with the same approach: the only difference is that the orbital electronic wave function of the pair of colliding atoms, being antisymmetric in the exchange of the spin-polarized electrons, is also, as a consequence, antisymmetric in the exchange of the protons alone. Because of this extra change of sign, Eq. (2) is replaced by

$$B_2^{2D}(\mathrm{H}\uparrow)=\langle P_T\rangle B_2^{2D+}+\langle P_S\rangle B_2^{2D-} . \tag{2'}$$

Formulas (2) and (2′) can be merged under the general form (equally valid for H↑):

$$B_2=\tfrac{1}{2}\langle 1+\epsilon\Pi\rangle B_2^{+}+\tfrac{1}{2}\langle 1-\epsilon\Pi\rangle B_2^{-} , \tag{3}$$

where Π is the nuclear-spin-permutation operator and where $\epsilon=+1$ in the bosonic case (H↑) and $\epsilon=-1$ in the fermionic cases (^{3}He, D↑).

Qualitative and quantitative effects of statistics are more easily discussed with the following alternative form of Eq. (3)

$$B_2=B_{2,\mathrm{dir}}+\epsilon\langle\Pi\rangle B_{2,\mathrm{exch}} \tag{4a}$$

with straightforward definitions of $B_{2,\mathrm{dir}}$ and $B_{2,\mathrm{exch}}$ in terms of B_2^{2D+} and B_2^{2D-}.

From the treatment of Ref. 26 transposed to the 2D case in Ref. 24, it is not difficult to establish the following expressions for $B_{2,\mathrm{dir}}^{2D}$ and $B_{2,\mathrm{exch}}^{2D}$ in terms of the two-dimensional scattering phase shifts $\delta_m(k)$ associated with the mth partial wave [see Appendix B for details about $\delta_m(k)$]

$$B_{2,\mathrm{dir}}^{2D}(T)=\frac{-\lambda^4}{\pi^2}\sum_{m=-\infty}^{+\infty}\int_0^{\infty}k\,dk\,\delta_m(k)\exp(-\beta\hbar^2k^2/2\mu) , \tag{4b}$$

$$B_{2,\mathrm{exch}}^{2D}(T)=\frac{-\lambda^2}{4}-\frac{\lambda^4}{\pi^2}\sum_{m=-\infty}^{+\infty}(-1)^m\int_0^{\infty}k\,dk\,\delta_m(k)\exp(-\beta\hbar^2k^2/2\mu) , \tag{4c}$$

where the phase shifts $\delta_m(k)$ are required to be continuous functions of the wave number k with the boundary conditions $\delta_m(0)=n\pi$ (n is the number of bound states with azimuthal quantum number m). Normally, the second virial coefficient also contains a contribution of the two-particle bound states. We have omitted it here because the best known H↑-H↑ potential does not allow any bound state. In the case of ^{3}He, the Aziz potential accomodates a bound state, but its binding energy is so weak (less than 10^{-5} K) that its contribution to Eqs. (4) is absolutely negligible in all regions of physical interest (see Appendix C).

In these equations, λ is the de Broglie wavelength of a H or ^{3}He atom of mass m at temperature T, $\lambda=h/(2\pi mk_BT)^{1/2}$ μ is the reduced mass of the relative particle, $\mu=m/2$.

Formula (4) calls for some general comments

(i) It is easily shown that

$$\frac{1}{2I+1}\le\langle\Pi\rangle\le 1 ,$$

the lower value being obtained for the unpolarized system and the higher one for the totally polarized one. In other words, nuclear polarization does reinforce the effects of quantum statistics.

(ii) For the spin-$\frac{1}{2}$ cases (H↑, ^{3}He)

$$\langle \Pi \rangle = \frac{1+M^2}{2} , \tag{5}$$

where M is the nuclear polarization $0 \leq M \leq 1$. The case of D↑ is in general more involved as it depends on two spin variables, the nuclear polarization, and alignment. Let us quote the result for the two extreme cases (zero or complete polarization)

$$B_2^{2D}(D\uparrow, M=0) = B_2^{2D-} , \tag{6a}$$

$$B_2^{2D}(D\uparrow, M=1) = \tfrac{2}{3} B_2^{2D-} + \tfrac{1}{3} B_2^{2D+} . \tag{6b}$$

(iii) The coefficient $B_{2,\mathrm{exch}}^{2D}$ has a physical meaning: It is directly related to the magnetic susceptibility χ in low magnetic field of a dilute nondegenerate gas. One can easily show (see for example Ref. 24):

$$(\chi - \chi_0)/\chi_0 = -\epsilon B_{2,\mathrm{exch}}^{2D}/S . \tag{7}$$

(iv) $B_{2,\mathrm{exch}}$ contains two contributions: The first one comes from the statistics of indistinguishable ideal particles. It is obviously negative at all temperatures so that the pressure of an ideal gas of bosons is always lower than that of an ideal gas of fermions. This is also true when the effect of the interparticle potential is taken into account (second contribution). It is a general property of 2D as well as 3D systems which has been demonstrated in Ref. 28. As an illustration, Tables I, II, and III show that $B_{2,\mathrm{exch}}^{2D}$ is negative for the three gases considered here.

(v) $B_{2,\mathrm{exch}}$, being an alternate function of the phase

TABLE I. Virial and spin-wave coefficients for H↑ vs temperature.

	H↑			
T (K)	$B_{2,\mathrm{dir}}^{2D}$ (Å^2)	$B_{2,\mathrm{exch}}^{2D}$ (Å^2)	μ	$D_0 n$ ($10^9 s^{-1}$)
0.01	2289.6	−5244.3	−2.51	2.44
0.02	1492.6	−2261.3	−2.31	4.20
0.03	1095.5	−1398.8	−2.17	5.65
0.04	870.49	−994.24	−2.07	6.93
0.05	725.54	−761.65	−1.99	8.11
0.06	624.04	−611.61	−1.93	9.20
0.07	548.82	−507.31	−1.87	10.24
0.08	490.72	−430.88	−1.82	11.22
0.09	444.43	−372.63	−1.78	12.15
0.1	406.65	−326.86	−1.74	13.04
0.12	348.57	−259.80	−1.67	14.72
0.14	305.94	−213.26	−1.61	16.29
0.16	273.27	−179.22	−1.56	17.76
0.18	247.38	−153.35	−1.51	19.16
0.20	226.36	−133.09	−1.46	20.50
0.24	194.22	−103.56	−1.39	23.02
0.28	170.78	−83.23	−1.32	25.37
0.32	152.90	−68.51	−1.26	27.58
0.36	138.80	−57.43	−1.21	29.70
0.40	127.39	−48.84	−1.16	31.73
0.50	106.50	−34.16	−1.06	36.50
0.60	92.32	−25.07	−0.97	40.94
0.70	82.05	−19.04	−0.89	45.13
0.80	74.26	−14.83	−0.83	49.13
0.90	68.14	−11.78	−0.77	52.96
1.00	63.22	−9.50	−0.71	56.65
1.20	55.76	−6.41	−0.62	63.66
1.40	50.39	−4.49	−0.54	70.25
1.60	46.34	−3.23	−0.47	76.48
1.80	43.16	−2.38	−0.41	82.42
2.00	40.62	−1.78	−0.36	88.09
2.40	36.77	−1.04	−0.28	98.75
2.80	34.02	−0.64	−0.22	108.66
3.20	31.94	−0.40	−0.18	117.96
3.60	30.32	−0.26	−0.14	126.74
4.00	29.02	−0.17	−0.12	135.09
10.00	21.85	-2.10^{-3}	−0.01	231.89
20.00	19.18	-3.10^{-4}	-10^{-3}	346.11
40.00	17.36		-2.10^{-4}	518.93
50.00	16.85			592.16

TABLE II. Virial and spin-wave coefficients for D↑ vs temperature.

	D↑			
T (K)	$B_{2,\mathrm{disc}}^{2D}$ (Å^2)	$B_{2,\mathrm{exch}}^{2D}$ (Å^2)	μ	$D_0 n$ ($10^9 s^{-1}$)
0.01	380.70	−3270.4	−7.89	18.04
0.02	197.79	−1563.3	−6.49	23.10
0.03	127.72	−1004.5	−5.52	24.66
0.04	90.95	−728.16	−4.82	25.02
0.05	68.39	−563.80	−4.30	24.95
0.06	53.22	−455.11	−3.90	24.75
0.07	42.39	−378.11	−3.57	24.54
0.08	34.32	−320.84	−3.31	24.35
0.09	28.11	−276.67	−3.09	24.20
0.10	23.22	−241.66	−2.91	24.10
0.12	16.08	−189.85	−2.62	24.02
0.14	11.23	−153.58	−2.39	24.09
0.16	7.80	−126.94	−2.21	24.27
0.18	5.32	−106.69	−2.06	24.54
0.20	3.48	−90.86	−1.93	24.87
0.24	1.07	−67.95	−1.73	25.69
0.28	0.30	−52.41	−1.57	26.65
0.32	−1.06	−41.36	−1.44	27.68
0.36	−1.44	−33.22	−1.33	28.77
0.40	−1.59	−27.08	−1.23	29.89
0.50	−1.39	−17.03	−1.03	32.75
0.60	−0.82	−11.25	−0.87	35.60
0.70	−0.13	−7.71	−0.75	38.38
0.80	0.59	−5.43	−0.64	41.07
0.90	1.29	−3.90	−0.55	43.67
1.00	1.96	−2.86	−0.48	46.19
1.20	3.16	−1.60	−0.36	50.95
1.40	4.21	−0.93	−0.27	55.41
1.60	5.13	−0.56	−0.21	59.61
1.80	5.92	−0.35	−0.16	63.59
2.00	6.63	−0.22	−0.13	67.39
2.40	7.80	−0.09	−0.08	74.51
2.80	8.74	−0.04	−0.05	81.12
3.20	9.52	−0.02	−0.04	87.32
3.60	10.17	−0.01	−0.03	93.20
4.00	10.71	-5.10^{-3}	−0.02	98.79
5.00	11.78	-10^{-3}	−0.01	111.79
6.00	12.55	-5.10^{-4}	-5.10^{-3}	123.70

shifts, rapidly goes to zero when the temperature increases: When more and more partial waves interfere, the collisions become quasiclassical and the effects of particle indistinguishability fade away.

B. Results and comments

Using the 2D scattering phase shifts $\delta_m(k)$ calculated as described in Appendix B, we computed the two contributions $B_{2,\mathrm{dir}}^{2D}(T)$ and $B_{2,\mathrm{exch}}^{2D}(T)$, as well as the total second virial coefficient $B_2^{2D}(T)$ for several values of the nuclear spin polarization, and for temperatures T between 0.1 and 50 K. The results are displayed in Fig. 1 and Table I for H↑, in Fig. 2 and Table II for D↑, and in Fig. 3 and Table III for ^{3}He.

TABLE III. Virial and spin-wave coefficients for ^{3}He vs temperature.

	^{3}He			
T (K)	$B_{2,\mathrm{dir}}^{2D}$ (Å^2)	$B_{2,\mathrm{exch}}^{2D}$ (Å^2)	μ	$D_0 n$ ($10^9 s^{-1}$)
0.01	−1032.1	−3444.5	2.53	2.79
0.02	−568.80	−1718.4	2.70	7.96
0.03	−389.38	−1118.0	1.55	15.55
0.04	−296.83	−815.55	2.02	24.98
0.05	−240.82	−634.19	1.16	34.68
0.06	−203.44	−513.72	0.16	42.70
0.07	−176.77	−428.14	−0.77	47.86
0.08	−156.80	−364.35	−1.49	50.24
0.09	−141.30	−315.10	−1.99	50.60
0.10	−128.91	−276.00	−2.31	49.78
0.12	−110.31	−218.04	−2.57	46.80
0.14	−96.97	−177.37	−2.59	43.75
0.16	−86.90	−147.45	−2.51	41.25
0.18	−78.99	−124.63	−2.41	39.34
0.20	−72.59	−106.74	−2.30	37.92
0.24	−62.77	−80.75	−2.09	36.16
0.28	−55.54	−62.99	−1.92	35.35
0.32	−49.93	−50.28	−1.77	35.14
0.36	−45.41	−40.86	−1.65	35.31
0.40	−41.67	−33.68	−1.54	35.74
0.50	−34.57	−21.78	−1.33	37.47
0.60	−29.48	−14.79	−1.16	39.72
0.70	−25.61	−10.41	−1.02	42.18
0.80	−22.54	−7.52	−0.90	44.73
0.90	−20.03	−5.55	−0.79	47.30
1.00	−17.94	−4.16	−0.70	49.85
1.20	−14.62	−2.44	−0.55	54.82
1.40	−12.10	−1.49	−0.44	59.58
1.60	−10.10	−0.94	−0.35	64.12
1.80	−8.48	−0.61	−0.28	68.45
2.00	−7.12	−0.40	−0.23	72.60
2.40	−4.99	−0.18	−0.15	80.41
2.80	−3.38	−0.09	−0.10	87.68
3.20	−2.11	−0.04	−0.07	94.51
3.60	−1.08	−0.02	−0.05	100.98
4.00	−0.23	−0.01	−0.04	107.13
5.00	1.37	−0.01	−0.02	121.43
6.00	2.50	-6.10^{-3}	-9.10^{-3}	134.51
10.00	4.93	-5.10^{-4}	-2.10^{-3}	179.20
20.00	6.88		-3.10^{-4}	265.31
40.00	7.76			395.54
50.00	7.88			450.46

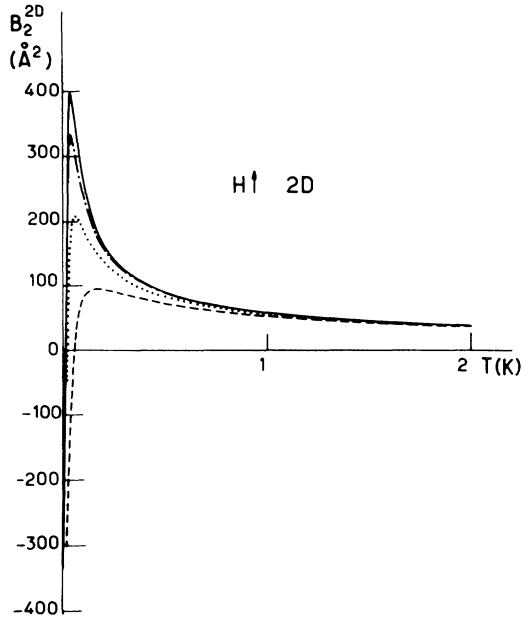

FIG. 1. Second virial coefficient B_2^{2D} of electronically-polarized hydrogen H↑ vs temperature —effect of its nuclear polarization M. ——, $M=0$; —·—·—·, $M=0.3$; · · · ·, $M=0.6$; — — —, $M=1$.

For these three systems, it is seen on Tables I, II, and III that the exchange contribution becomes significant around 1 K and below. This comes from a counterbalance between the pure quantum-statistics term and the interaction contribution. Above 2 K, exchange effects be-

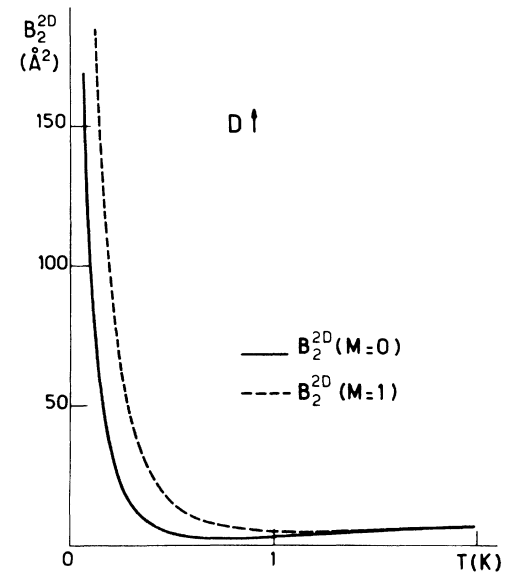

FIG. 2. Second virial coefficient of D↑ vs temperature. ——, $M=0$: $B_2^{2D}(D\uparrow)=B_{2,\mathrm{dir}}^{2D}-\frac{1}{3}B_{2,\mathrm{exch}}^{2D}$; — — —, $M=1$: $B_2^{2D}(D\uparrow)=B_{2,\mathrm{dir}}^{2D}-B_{2,\mathrm{exch}}^{2D}$.

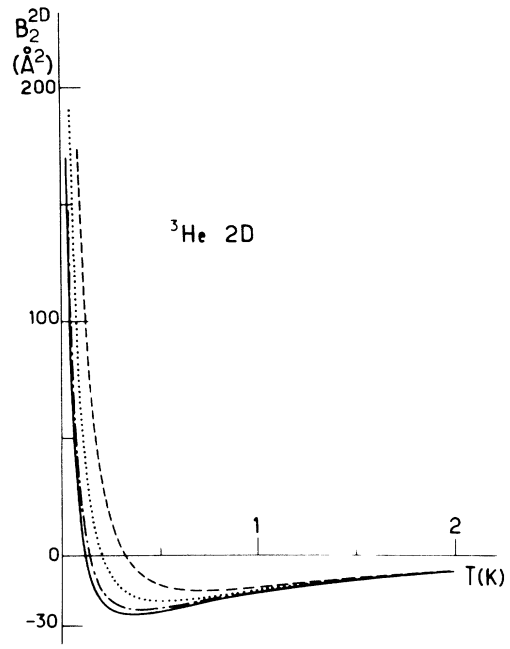

FIG. 3. Second virial coefficient B_2^{2D} of ^{3}He vs temperature —effect of the nuclear polarization. ——, $M=0$; —·—·—·, $M=0.3$; · · · ·, $M=0.6$; — — —, $M=1$.

come negligible and the virial coefficient is dominated by $B_{2,\mathrm{dir}}^{2D}$. Although of restricted physical interest, the computation of B_2^{2D} above 10 K shows that the virial coefficient approaches the semiclassical value $(\pi\sigma^2/2)$ of a gas of hard disks of radius σ.

The role of the nuclear polarization appears in Figs. 1, 2, and 3. As expected it is noticeable at low temperatures as soon as the exchange contribution manifests itself. The weight of the quantum exchange term increases with the nuclear polarization and the fact that $B_2^{2D}(M=1)$ stands below $B_2^{2D}(M=0)$ for H↑ and above $B_2^{2D}(M=0)$ for ^{3}He and D↑ is a mere illustration of the attractive or repulsive character of Bose-Einstein or Fermi-Dirac statistics.

Although we have neglected here the influence of a substrate of H_2 or ^{4}He on which experiments are usually done, its effect on B_2^{2D} should be rather small. The M dependence of B_2^{2D} displayed here should lead to a nuclear-polarization-dependent coverage of H↑, D↑, or ^{3}He atoms on the surface. Whereas the nuclear polarization should favor the adsorption of H↑ atoms, polarized ^{3}He atoms tend to be excluded from the surface with respect to unpolarized ^{3}He atoms. (The latter is also true to D↑.) This effect might be used experimentally to enhance the nuclear polarization of the bulk vapor.

For H↑, we compared our results with those of Ref. 25. The unphysical behavior of the quantum statistics effects in this reference probably explains most of the 10% disagreement with our results.

For ^{3}He, we compared our results to the leading work of Siddon and Schick.[24] These authors computed the two-dimensional virial coefficient of unpolarized ^{3}He ($M=0$), using the Lennard-Jones 6-12 potential fitted to ^{3}He. This potential has a smaller well depth (10.22 K instead of 10.8 K) and a smaller hard core (2.55 Å instead of 2.63 Å) than the Aziz potential of Ref. 29 that we used here. It is thus not surprising that the virial coefficient listed in their work, though in good agreement at high temperatures, lies roughly 30% above our values where B_2 is minimum. This disagreement is explained by the long-recognized sensitivity of B_2 in this region to the details of the potential, near the minimum of the well.

III. SPIN-WAVE CHARACTERISTIC COEFFICIENTS IN TWO DIMENSIONS

A. Formalism

Because spin waves originate from indistinguishability effects occurring during a binary collision, it is possible to derive their characteristics from the quantum Boltzmann equation established in Ref. 11 for nondegenerate bosons (or fermions). This equation which has the same form in two and three-dimensions describes the evolution under the effect of binary collisions of the spin-density operator.

In the restricted range of validity of the Boltzmann equation, i.e., in the range of temperature and density where the molecular-chaos assumption is legitimate, there is no special pathology associated with the Boltzmann equation in 2D. Difficulties with regards to a transport equation in 2D arise for increasing density when the molecular-chaos assumption breaks down, urging for the taking into account of various memory effects. When these effects can be neglected, it is possible, like in 3D, to introduce the so-called spin-diffusion coefficient defined as the proportionality coefficient between the current of magnetization driven by the gradient of the nuclear polarization **M**. As well as in 3D diffusion, the parallel and transverse components of **M** behave quite differently. For a given polarization $M_z=M$, the general form of the polarization current is

$$\mathbf{J}(M_z)=-D_0\nabla M_z\ , \tag{8a}$$

$$\mathbf{J}(M_x)=-D_\perp(\nabla M_x+\epsilon\mu M\nabla M_y)\ , \tag{8b}$$

$$\mathbf{J}(M_y)=-D_\perp(-\epsilon\mu M\nabla M_x+\nabla M_x)\ . \tag{8c}$$

It is clear on these equations that μ governs the efficiency of exchange effects to create an oscillatory response of the gas to gradients of its polarization, whereas D_0 and $D_\perp$ reflect the damping of these spin waves. We refer the reader to Ref. 11 for further comments on these equations.

The coefficients D_0, $D_\perp$, and μ can be expressed with the help of collision integrals involving various angle-averaged cross sections given in Appendix A. A good approximation of these coefficients is then

$$D_0=\frac{16m^2}{\beta^3 n_a(2\hbar^5)}\left[\int_0^\infty k^4dk\,e^{-\beta\hbar^2k^2/m}Q_{[\sigma_k]}\right]^{-1}\ , \tag{9a}$$

$$\mu=\frac{\int_0^\infty k^4dk\,e^{-\beta\hbar^2k^2/m}[Q_{[\tau_k^{\mathrm{ex}}]}+\tau_{\mathrm{fwd}}^{\mathrm{ex}}]}{\int_0^\infty k^4dk\,e^{-\beta\hbar^2k^2/m}Q_{[\sigma_k]}}\ , \tag{9b}$$

$$D_\perp=D_0/(1+\mu^2M^2)\ , \tag{9c}$$

(n_a is the two-dimensional number density of the gas, β is defined as $1/k_B T$, and k_B is the Boltzmann constant).

The angle averaged cross-sections are defined as

$$Q_{[\sigma_k]}(k)=\int_0^{2\pi} d\theta(1-\cos\theta)\sigma_k(\theta) = \frac{2}{k}\sum_{m=-\infty}^{+\infty}\sin^2(\delta_m-\delta_{m+1}) , \quad (10a)$$

$$Q_{[\tau_k^{ex}]}(k)=\int_0^{2\pi} d\theta(1-\cos\theta)\tau_k^{ex}(\theta) = \frac{1}{k}\sum_{m=-\infty}^{+\infty}(-1)^m\{\sin[2(\delta_{m+1}-\delta_m)] + 2\sin(2\delta_m)\} , \quad (10b)$$

which, combined with (9c), leads to

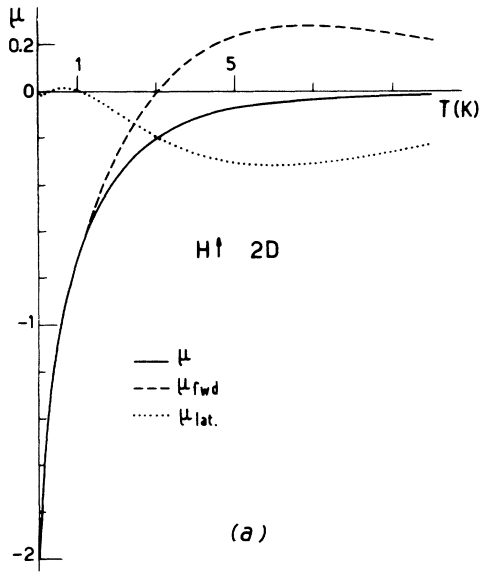

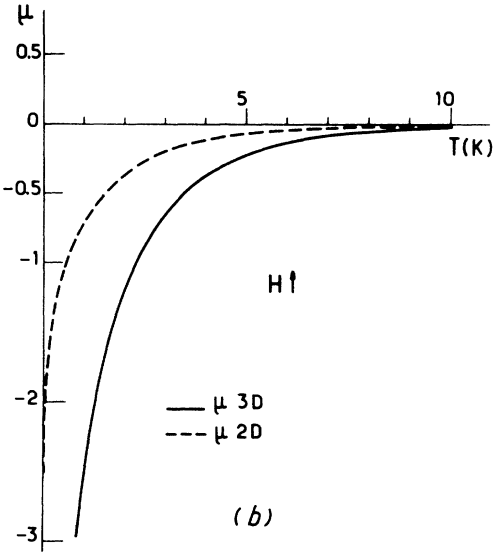

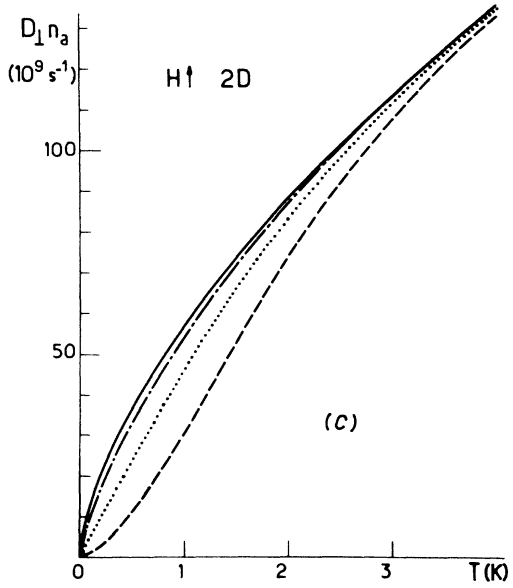

FIG. 4(a) μ for H↑ in two dimensions as a function of temperature. The two contributions μ_{fwd} and μ_{lat} are also shown to throw light on the validity of the molecular approximation. (b) Comparison between the coefficients μ in 2D and 3D for H↑. (c) Transverse spin diffusion coefficient $D_\perp n_a = D_0 n_a/(1+\mu^2 M^2)$ for several nuclear polarizations of H↑. The $M=0$ case gives the longitudinal spin diffusion coefficient. ——, $M=0$; —·—·—·, $M=0.3$; · · · ·, $M=0.6$; — — —, $M=1$.

$$Q_{[\tau_k^{ex}]}+\tau_{fwd}^{ex}=\frac{2}{k}\sum_{m=0}^{\infty}(-1)^m\sin[2(\delta_m-\delta_{m+1})]\ . \qquad (10c)$$

The above expressions call for two comments.

(i) They can be simplified in some cases by neglecting the $Q_{[\tau^{ex}]}$ contribution. From a physical point of view this amounts to neglecting the coherent lateral scattering. Going further and leaving out all the phase shifts other than δ_0 leads to

$$\mu=\frac{1}{2}\frac{\int_0^\infty k^3dk\,e^{-\beta\hbar^2k^2/m}\sin(2\delta_0)}{\int_0^\infty k^3dk\,e^{-\beta\hbar^2k^2/m}\sin^2\delta_0} \qquad (10d)$$

(which incidentally takes the same form as in three dimensions). It is the kind of approximation done in the "molecular-field" approaches.[3,5,,12,17,30] Justified in the case of weak interactions, at sufficiently low temperature, this approximation can break in the intermediate temperature range. One of the aims of the present calculation is to set the limit of validity of this approximation in the 2D case.

(ii) Most of the differences between the 2D and 3D cases will originate from the low-energy s-wave phase-shift behavior as will be discussed in detail below.

B. Spin diffusion in 2D polarized quantum gases: Results and comments

Before discussing the specific characters of these coefficients for H↑, D↑, and ^{3}He, we wish to comment on some common features which emerge from our results shown in Figs. 4–6 and Tables I–III.

First, it can be noticed from Figs. 4(b), 5(a), 5(b), and 6(b) that "quantum exchange effects," from which μ originates, appear at lower temperatures in 2D than in 3D. The physical explanation of this feature is the following: The "negative centrifical barrier" which enters the 2D Schrödinger equation [see Appendix B Eq. (B3)] has sizable effects at intermediate distances where it can be viewed as an increase of the mass of the particle under study. This makes a two-body collision, at intermediate energies, more "classical" and tends to reduce its quantum nature. (In Appendix C, we give some orders of magnitude of this negative barrier compared to the actual interaction potential.) This character of 2D scattering explains why the spin-wave quality factor μ becomes significant at lower temperatures than in 3D. This feature also influences the anisotropy of the spin diffusion coefficient (measured by $D_0/D_\perp=1+\mu^2M^2$) which appears on Figs. 4(c) and 6(c).

We also show on Figs. 4(a) and 6(a) an analysis of the various contributions to μ originating, respectively, in coherent, lateral, and backward-forward scattering. These figures allow to specify the validity of a "molecular-field" type of approximation which neglects the effects of lateral scattering. This approximation overestimates quantum exchange effects and it can lead to appreciable errors on the magnitude of μ in the temperature range of experimental interest. This restriction of validity appears more markedly in 2D than in 3D (Ref. 31) since two dimensionality is less favorable to quantum exchange as already discussed above.

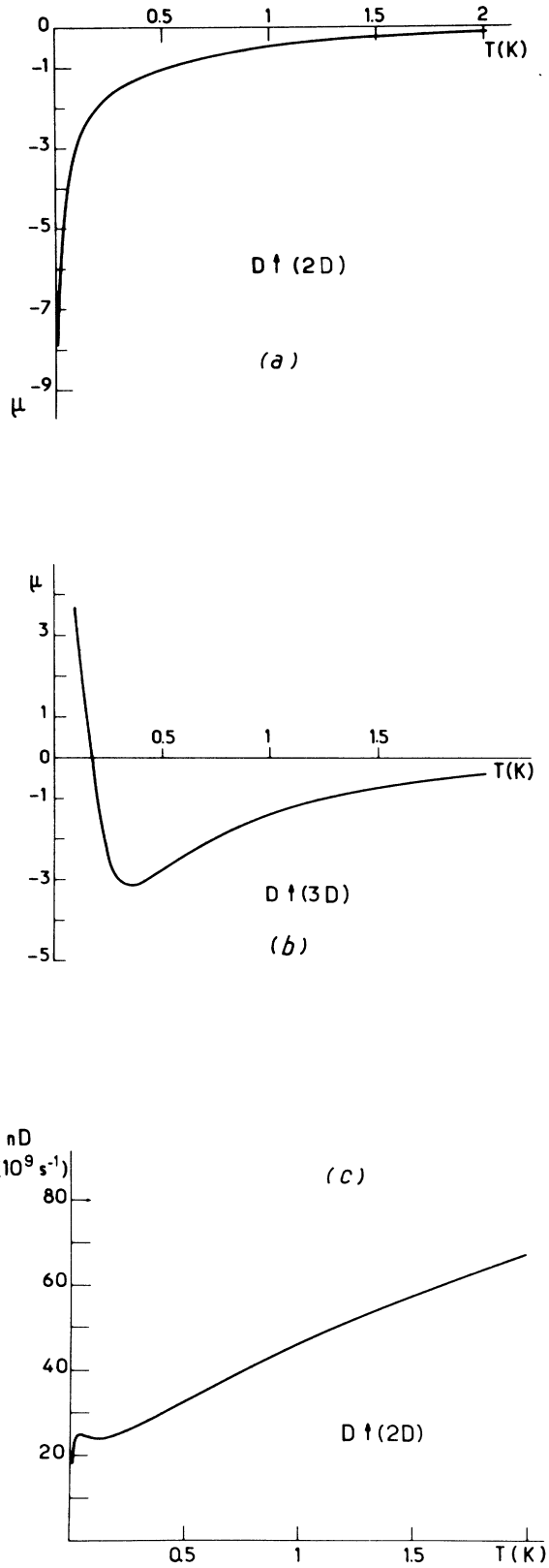

FIG. 5(a) μ for D↑ in two dimensions as a function of T. (b) μ for D↑ in three dimensions as a function of T. (c) Longitudinal spin diffusion coefficient of D↑ in two dimensions.

Our results all together allow discussion of the possibility of dimensional or mass scaling that was used by Bashkin[16] and discussed at the beginning of this article. For instance, it is possible to define from the longitudinal spin-diffusion coefficient D_0 an average cross section of collision $\bar{Q}^1_{[\sigma_k]}$ in three and two dimensions (for which this quantity is actually a length). At 4K in 3D, this average cross section is found from Ref. 11 to be 40 Å^2 for H↑ and 23 Å^2 for ^{3}He, whereas in 2D, we find an average cross length of 6.7 Å for H↑ atoms and 4.6 Å for ^{3}He at 4 K. These values are therefore in good agreement from a naive dimensional analysis. Besides, Table II leads to a cross length of 6.4 Å for D↑ atoms at 4 K which shows that a change of the mass has a small effect and that this cross length is mainly determined by the interaction potential which is the same for the two isotopes.

This is no longer true at low temperatures where dimensional or mass scaling appears to be bound to failure because the properties of light quantum gases result from a delicate balance between interaction and quantum exchange effects. The spin-wave quality factor μ of deuterium atoms is a striking example of this statement since the

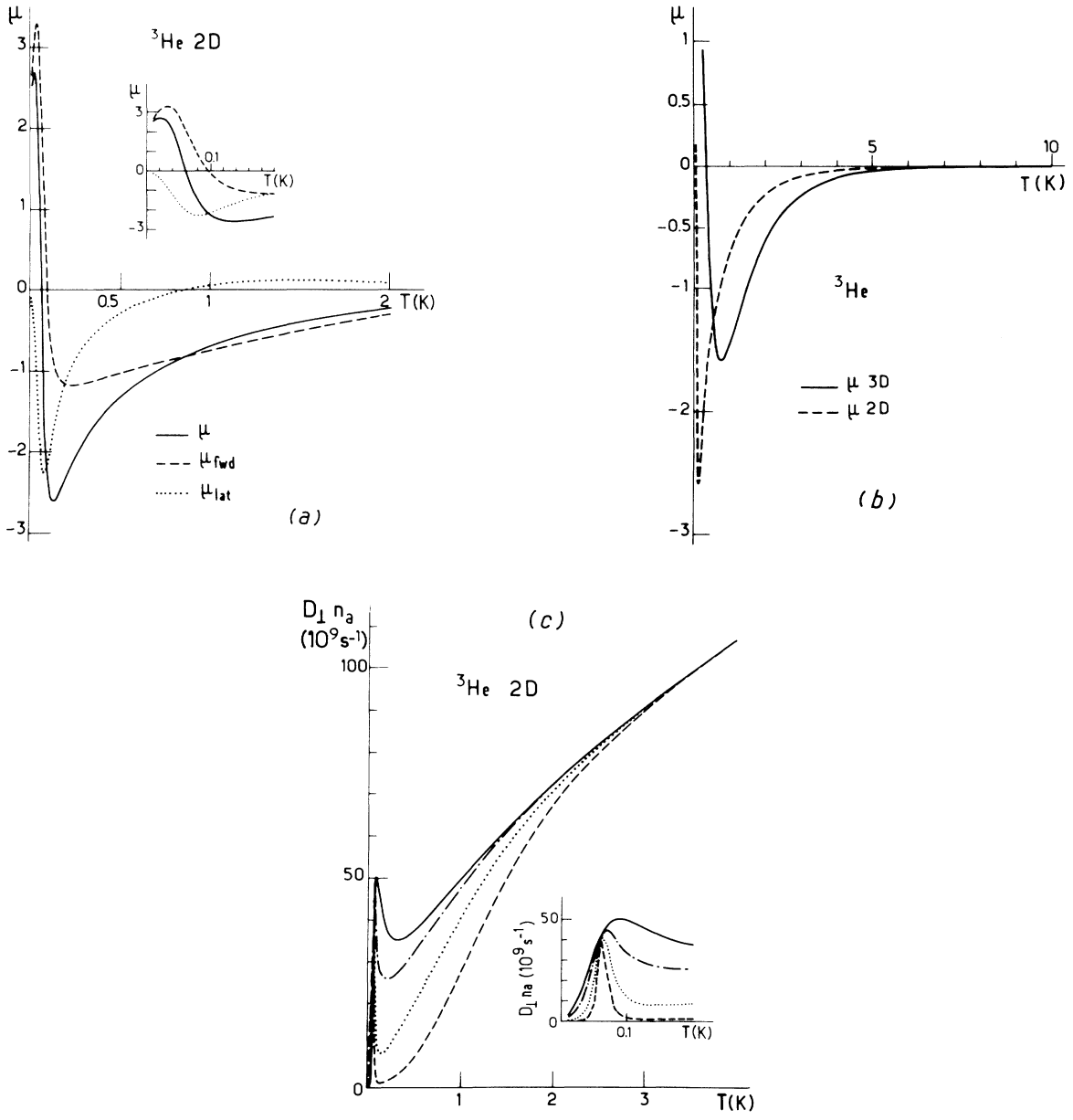

FIG. 6(a) μ for ^{3}He in two dimensions as a function of temperature [same comment as in Fig. 3(a)]. (b) Comparison between μ in 2 and 3D for ^{3}He. (c) Transverse spin diffusion coefficient $D_\perp na = D_0 na/(1+\mu^2 M^2)$ for several nuclear polarizations of ^{3}He. The $M=0$ case gives the longitudinal spin diffusion coefficient. ——, $M=0$; —·—·—·, $M=0.3$; · · · ·, $M=0.6$; — — —, $M=1$.

shape of $\mu(T)$ is completely different in 2D and 3D. [See Figs. 5(a) and 5(b).]

We now turn to specific comments for each of the gases studied.

(a) H↑

Our results must be compared to those of Koelman *et al.*[17] As discussed in the introduction, the model of these authors is more sophisticated and more physical than ours insofar as it takes partially into account the z extension of the wave function ($2\frac{1}{2}$ D model). On the other hand, they used an s-wave approximation that should be checked at intermediate temperatures. The comparison between the two sets of data and the detailed analysis of our results show that the s-wave approximation is entirely valid up to 500 mK, that is in most of the experimental range of interest. Above this temperature, contributions other than the s wave cannot be disregarded.

(b) D↑

Spin-polarized deuterium is a very good illustration of the dramatic changes that dimensionality can induce in the properties of a quantum gas. This was already pointed out just above but it deserves some further comments. The comparison of Fig. 5(a) and (b) showing μ in two and three dimensions gives an opportunity to discuss under what conditions μ is positive at low temperatures. From Eq. (10d), this obviously happens when $0<\delta_0<\pi/2$. In 3D, such behavior is encountered in D↑ and ^{3}He for which the effect of the interaction is weakly attractive at low energy. In 2D, the scattering phase shift δ_0 becomes positive only when it goes to π when k tends to 0, that is to say, when there is a bound state. This is due to the logarithmic behavior of $\delta_0(k)$ which forbids the scattering length to be negative or, equivalently, the slope of $\delta_0(k)$ to be positive.[32] This specific feature of 2D scattering explains why μ remains negative for D↑ atoms in 2D; while the slightly attractive potential is able to yield a positive low energy $\delta_0(k)$ in 3D, it is yet not strong enough to sustain a bound state in 2D so that this phase shift remains negative and tends toward zero when $k\rightarrow 0$.

(c) ^{3}He

The ^{3}He case is precisely an example where the existence of a loosely bound state ($E_b<10^{-5}$ K) leads to positive values of μ at low temperatures as seen in Fig. 6(a). In fact, from a physical point of view, it appears that a measurement of μ would be an extremely sensitive test of the quality of the interatomic potential as it could sign unambiguously the existence, in a real physical situation, of a two-dimensional bound state.

It appears in Fig. 6(b) that the range of temperature where μ is measurable is shifted from around 2 K in 3D down to 1 K in 2D. This phenomenon was explained to be due to the more "classical" behavior of quantum gases in 2D, at intermediate temperatures. However, this does not prevent the minimum of μ to be more pronounced in 2D than in 3D.

The transverse spin diffusion represented in Fig. 6(c) for different values of the nuclear polarization M, exhibits a peak around 0.1 K. It is a remainder of the quantum oscillations of the cross section $\sigma_k(\theta)$ due to the diffraction by the interaction potential. This feature is visible for all polarizations. It is more contrasted for $M=1$ since interference effects then affect both σ_k and $\tau_{\text{fwd}}^{\text{ex}}$. As a result, spin diffusion is strongly anisotropic in this temperature range.

The results presented here and their comparison with the 3D counterpart show that experimental measurements on spin waves in a ^{3}He vapor can be affected by the behavior of the nuclear polarization in the adsorbed phase from 2 K and below. However, quantitative predictions about this effect require an elaborate model for the coupling of the adsorbed and bulk phases. Moreover, measurements on the vapor[15] are probably more sensitive to "classical" effects induced by the magnetization of an adsorbed ^{3}He layer. In order to check the existence of two-dimensional spin waves in ^{3}He, it seems more adequate to design an experiment where most of the ^{3}He atoms are adsorbed by using a sample with very large surface volume ratio. Such an experiment would also require high quality substrate to avoid the damping of spin waves by the diffusion of ^{3}He atoms by defects or impurities.

IV. CONCLUSION

We have computed the virial coefficients and spin diffusion coefficient of H↑, D↑, and ^{3}He in two dimension and their dependence on the nuclear polarization. This dependence—entirely related to statistics—becomes noticeable in the Kelvin range and below. The results for coefficients which do not depend on statistics (D_0,B_{dir}) have been extended up to 50 K.

As a general qualitative feature, the weight of quantum exchange effects tends to be reduced with decreasing dimensionality. Moreover, the specific "more classical" behavior of 2D dynamics which explains the existence of a two-dimensional dimer of ^{3}He, for example, equally contributes to the decrease of the exchange effects in 2D versus 3D.

Finally, we have shown to what extent and why mass scaling or dimensional scaling is inefficient to estimate the order of magnitude and sometimes even the sign of the statistical effects. The results presented here show that, on the contrary, a detailed knowledge of the phase shifts is generally required to compute these coefficients.

ACKNOWLEDGMENTS

The authors are very grateful to F. Laloë, J. Dupont-Roc, and J. Vigué for valuable and fruitful discussions, and to O. E. Vilches for his interest in this work. The Laboratoire de Spectroscopic Hertzienne is Laborataire associé au Centre National de la Recherche Scientifique, LA 18.

APPENDIX A: 2D COLLISIONAL CROSS SECTIONS AS FUNCTIONS OF THE T-MATRIX ELEMENTS AND SCATTERING PHASE SHIFTS

In this appendix, we want to summarize the relevant formulas for the description of exchange effects in spin-polarized gases in two dimensions. We shall not develop here the theory of quantum scattering in two dimensions,

and refer the reader to didactical papers which cover most of the features of interest.[33–35] Nor shall we repeat the detailed analysis of a collision between particles with internal degrees of freedom given in Ref. 11. Like in three dimensions, the description of a collision taking into account indistinguishability effects involves four independent real numbers that we call "cross sections" (although in 2D these quantities have actually the dimension of a length) and which can be expressed in terms of the transition matrix elements $T_k(\hat{\mathbf{k}}_i,\hat{\mathbf{k}}_f)$. From the knowledge, in the two-dimensional case of the relation between $T_k(\hat{\mathbf{k}}_i,\hat{\mathbf{k}}_f)$ and the phase shifts $\delta_m(k)$:

$$T_k(\hat{\mathbf{k}}_i,\hat{\mathbf{k}}_f)=\frac{i}{\mu}\sum_{m=-\infty}^{+\infty} e^{im\theta}(e^{2i\delta_m}-1) .$$

[$\mathbf{k}_i$ and $\mathbf{k}_f$ are the initial and final momentum vectors; because the energy is conserved, the T-matrix elements depend only on $k=|\mathbf{k}_i|=|\mathbf{k}_f|$ and on θ, the angle between $\hat{\mathbf{k}}_i$ and $\hat{\mathbf{k}}_f$. It is then easy to derive the following expressions of the four real cross sections σ_k, $\sigma_k^{\rm ex}$, $\tau_k^{\rm ex}$, and $\tau_{\rm fwd}^{\rm ex}$ as functions of the two-dimensional phase shifts $\delta_m(k)$:

$$\sigma_k(\theta)=\frac{8\pi^3\mu^2}{\hbar^4 k}|T_k(\hat{\mathbf{k}}_i,\hat{\mathbf{k}}_f)|^2$$
$$=\frac{1}{2\pi k}\sum_{m,m'} e^{i(m-m')\theta}(e^{2i\delta_m}-1)(e^{-2i\delta_{m'}}-1) ,$$

$$\sigma_k^{\rm ex}(\theta)-i\tau_k^{\rm ex}(\theta)=\frac{8\pi^3\mu^2}{\hbar^4 k}T_k(-\hat{\mathbf{k}}_f,\hat{\mathbf{k}}_i)T_k^*(\hat{\mathbf{k}}_f,\hat{\mathbf{k}}_i)$$
$$=\frac{1}{2\pi k}\sum_{m,m'} e^{i(m-m')\theta}(-1)^m \times(e^{2i\delta_m}-1)(e^{-2i\delta_{m'}}-1) ,$$

$$\tau_{\rm fwd}^{\rm ex}=\frac{-4\pi^2\mu}{\hbar^2 k}[T_k(-\hat{\mathbf{k}}_i,\hat{\mathbf{k}}_i)+T_k^*(-\hat{\mathbf{k}}_i,\hat{\mathbf{k}}_i)]$$
$$=\frac{2}{k}\sum_m(-1)^m\sin(2\delta_m) ,$$

where the azimuthal quantum numbers m and m' vary between $-\infty$ and $+\infty$. As a consequence of their specific k dependence and of the logarithmic behavior of δ_0, these 2D cross sections diverge at low energy.

APPENDIX B: 2D PHASE SHIFTS OF H↑, D↑, AND ^{3}He

To introduce and comment on our results on the two-dimensional shifts of H↑, D↑, and ^{3}He it seems useful to collect and recall the analytical results that have been obtained in various limiting situations.

1. Some analytical results

a. Hard-disk phase shifts

It is straightforward to show that the phase shifts for the hard-disk potential (with radius size R_c) are determined mod($n\pi$) by

$$\tan\delta_m=\frac{J_m(kR_c)}{N_m(kR_c)} .$$

At high energy ($kR_c\gg1$), these phase shifts are given by

$$\delta_m\simeq -kR_c+\frac{\pi}{2}(m-\tfrac{1}{2}) .$$

On the other hand, their behavior at low energy ($kR_c\ll1$) is

$$\tan\delta_0=\frac{\pi}{2}\frac{1}{\ln(kR_c/2)+C}+O(k^2) ,$$
$$\tan\delta_m=\frac{-\pi}{m!(m-1)!}\left[\frac{kR_c}{2}\right]^{2m}+\cdots \quad \text{for } m\neq0 , \tag{B1}$$

where $C=0.577215\ldots$ is Euler's constant.

Equation (B1) highlights the specificity of 2D scattering. Whereas, in 3D the s-wave phase shift for a hard-core potential would be everywhere equal to $-kR_c$ this phase shift in 2D tends logarithmically slowly towards 0. Although its derivative tends to infinity, this phase shift is always greater in magnitude than kR_c.

b. Scattering length and effective-range theory

After some controversy it has recently been shown (Refs. 17, 36, 37, and references therein) that for any finite-range potential, the low energy behavior of δ_0 can be approximated by

$$\text{cotan}\delta_0=\frac{2}{\pi}\left[\ln\frac{ka}{2}+C\right]+\frac{r_e k^2}{2\pi} , \tag{B2}$$

where a is the scattering length and r_e the effective range in two dimensions. Contrary to the three-dimensional case where positive and negative infinite values of the scattering length equivalently signal the appearance of a bound state, here in two dimensions the scattering length is always positive. The existence of a loosely bound state is accompanied by the abrupt change of a from 0 to $+\infty$.

Certainly valid at sufficiently low energy, and for weak potentials the open question raised by this approach, is its numerical range of validity in a case of a not-too-weak potential. The quantum phase-shift calculation done below will give a pragmatic answer to this question.

2. 2D Phase shifts of H↑, D↑, and ^{3}He

The interaction potential between H↑ or D↑ atoms was chosen to be the fit to the Kolos-Wolniewicz potential[38] given by Silvera.[39] As for ^{3}He the interaction potential is the fit obtained by Aziz *et al.*,[29] since it remains, to our knowledge, the best potential for He up to date.

In order to calculate the phase shifts, it is necessary to solve the radial Schrödinger equation. For that purpose, it is convenient to define a reduced radial wave function $v_m(r)=\sqrt{r}R_m(r)$ which obeys the following equation

$$-\ddot{v}_m+\frac{(m^2-1/4)}{r^2}v_m+(U-k^2)v_m=0 . \tag{B3}$$

For the sake of comparison, we recall here that in 3D, $v_m=rR_m(r)$ would satisfy

$$-\ddot{v}_m + \frac{l(l+1)}{r^2} v_m + (U - k^2) v_m = 0 \ . \qquad \text{(B4)}$$

This shows that the only significant differences between two and three dimensions are expected for low values of the angular momentum and especially for $m=0$, in the region $kr \lesssim 1$.

The scattering phase shifts were computed after a numerical integration of Eq. (B3) according to the standard Runge-Kutta procedure. The results are reported in Figs. 7, 8 and 9, as functions of the reduced wave number $k^*=k\sigma$ [with σ defined by $V(\sigma)=0$]. We only show here the phase shifts up to $k^*=7$, but they were computed between $k^*=1/6300$ and $k^*=14$. In Figs. 7, 8, and 9, we chose to represent the phase shifts between $-\pi/2$ and $+\pi/2$. However, it is important in the calculation of the virial coefficient to take into account the requirement that the phase shifts should be continuous functions of the wave number. This is easily done by subtracting π each time a phase shift reaches $-\pi/2$.

a. H↑

At first sight, hydrogen phase shifts seem a very good illustration of a purely repulsive hard-core potential. The s-wave phase shift δ_0 closely resembles the logarithmic behavior described by Eq. (B1) (see Fig. 7).

However, phase shifts for $m \neq 0$ show a noticeable contribution of the weak attractive potential in the region where they are positive. Besides, the scattering length $a=1.1$ Å derived from our results in agreement with the value given in Ref. 17, is much smaller than the core radius $\sigma=3.68$ Å. This is also attributed to the attractive part of the potential.

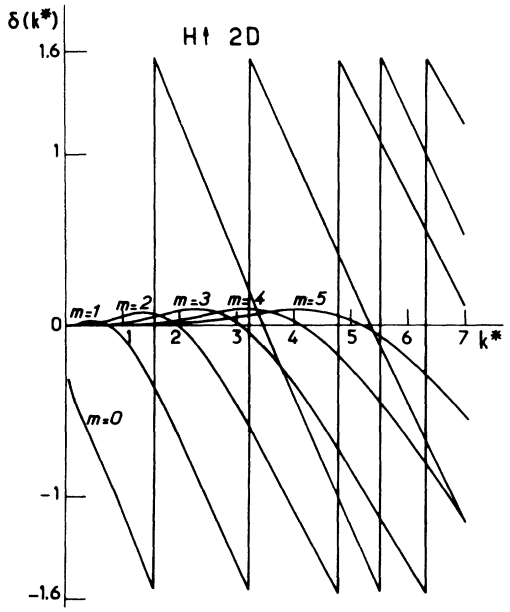

FIG. 7. 2D scattering phase shifts for H↑ calculated from the Silvera triplet potential, (Ref. 8) as a function of the reduced wave number $k^*=k\sigma$ ($\sigma=3.687$ Å).

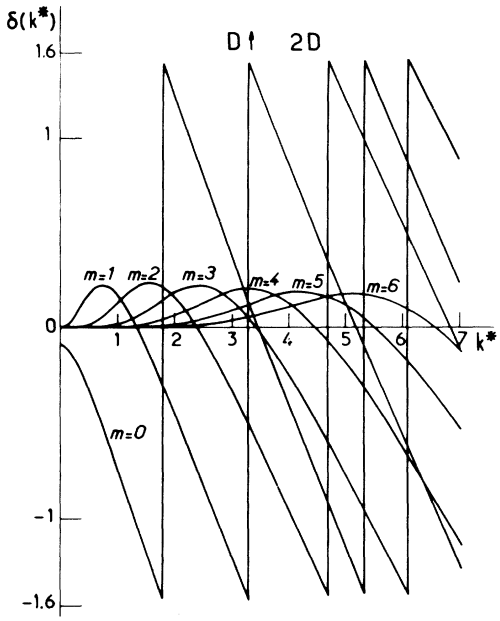

FIG. 8. 2D scattering phase shifts for D↑ calculated from the Silvera triplet potential as a function of the reduced wave number $k^*=k\sigma$ ($\sigma=3.687$ Å).

Accidentally, it happens that the scattering length has nearly the same magnitude in two and three dimensions (0.72 Å in 3D, see Ref. 11). It is then clear that $\delta_0 \simeq -ka$ in 3D is smaller in magnitude than $\delta_0 \sim \pi/2$ ln $(ka/2)$ in 2D, when $ka \ll 1$. This is essential to the behavior of B_2^{2D}, μ, and D_0.

b. D↑

The heavier mass of deuterium produces significant changes in the phase shifts. As expected, the attractive well of the potential exerts a stronger influence than for H↑. This is why the phase shifts other than δ_0 are markedly positive at low energy (see Fig. 8). Moreover, the scattering length $a \sim 2\times 10^{-5}$Å is very close to zero. This indicates that the interaction potential is nearly strong enough to sustain a bound state.

c. ^{3}He

It can be seen in Fig. 9(b) that the s-wave phase shift at low energy reaches $\pi/2$ at $k_0^*=1.83\times 10^{-3}$. This is the signature of the existence of a bound state. It also means that by continuity, $\delta_0(0)$ is equal to π according to Levinson's theorem. Besides, the wave number k_0^* at which $\delta_0=\pi/2$ corresponds to the energy of the loosely bound state $E_B=-\hbar^2 k_B^2/2\mu$.

This feature is a specific property of two-dimensional scattering which can be demonstrated in the simple case of a potential $V(r)$ defined by

$$V(r)=\pm\infty \quad \text{for } r<\sigma\text{: region I ,}$$

$$V(r)=-V_0=-\hbar^2\mathcal{K}_0^2/2\mu \quad \text{for } \sigma<r<R\text{: region II ,}$$

$$V(r)=0 \quad \text{for } r>R\text{: region III ,} \qquad \text{(B5)}$$

which has the essential characteristics of a realistic potential, namely a strong hard core repulsion at short distances and an attractive well at intermediate distances).

We assume here that kR, k_BR, $\mathcal{H}_0R \ll 1$ in order to describe a situation where this potential barely sustains a bound state. The principle of the demonstration is very simple; it is based on the matching conditions at $r=\sigma$ and $r=R$ of both solutions: the weakly bound state (assumed to exist) and the $m=0$ diffusion state with energy $\hbar^2k^2/m$. Because, as a first approximation, the wave function in region II has the same shape for these two states, these matching conditions allow to relate the low-energy phase shift $\delta_0(k)$ to the binding energy by the following formula

$$\tan\delta_0 = \frac{\pi/2}{\ln(k/k_B)} \ . \tag{B6}$$

It is obvious in (B6) that within the approximation used here, δ_0 is equal to $\pi/2$ for $k_0=k_B$. Besides, it follows immediately from (B6) that the scattering length as defined by (B2) is simply equal to

$$a = 2\exp(-C)/k_B = (1/k_B)(1.12) \ . \tag{B7}$$

Equation (B6) clearly assumes the existence of a bound state. This requires a threshold condition to be satisfied, which will be discussed with more details in Appendix C [see Eq. (C4)].

Returning to the case of ^{3}He, the results of our computation of δ_0 are well described by this simple model at energies comparable to the binding energy. The scattering length derived with the help of (B2) from the values of δ_0 at low energy is 1560 Å within a few percent. Besides, this phase shift is equal to $\pi/2$ at $k_B^* = 1.83\times10^{-3}$ which gives, from (B7), a scattering length of 1570 Å. Moreover, these values are also in good agreement with the binding energy of about -0.9×10^{-5} K presented below. (Although it is not shown here, we also computed the phase shifts of ^{4}He in two dimensions. For the s wave, δ_0 exhibits a similar behavior as compared to ^{3}He, except, of course, that the scattering length 24 Å is shorter, which agrees with the much higher binding energy of about -36 mK, given in Appendix C).

Being very small the exact value of the binding energy is of little interest in any realistic experimental situation. Nevertheless, as it was noticed earlier, it is the mere existence of this loosely bound state that determines μ to be positive up to 60 mK.

This study shows that light quantum gases cover a wide range of scattering lengths. While H↑ is well described by a scattering length theory, D↑ and ^{3}He are two extreme cases, just below and above the threshold for binding; consequently, their scattering lengths (2.10^{-5}Å for D↑ and 1570 Å for ^{3}He) are extremely sensitive to small changes of the potential and are only useful in a very restricted range of temperature. One must therefore conclude that a numerical computation of the phase-shifts cannot be avoided in order to get reliable predictions about virial and transport coefficients in these systems.

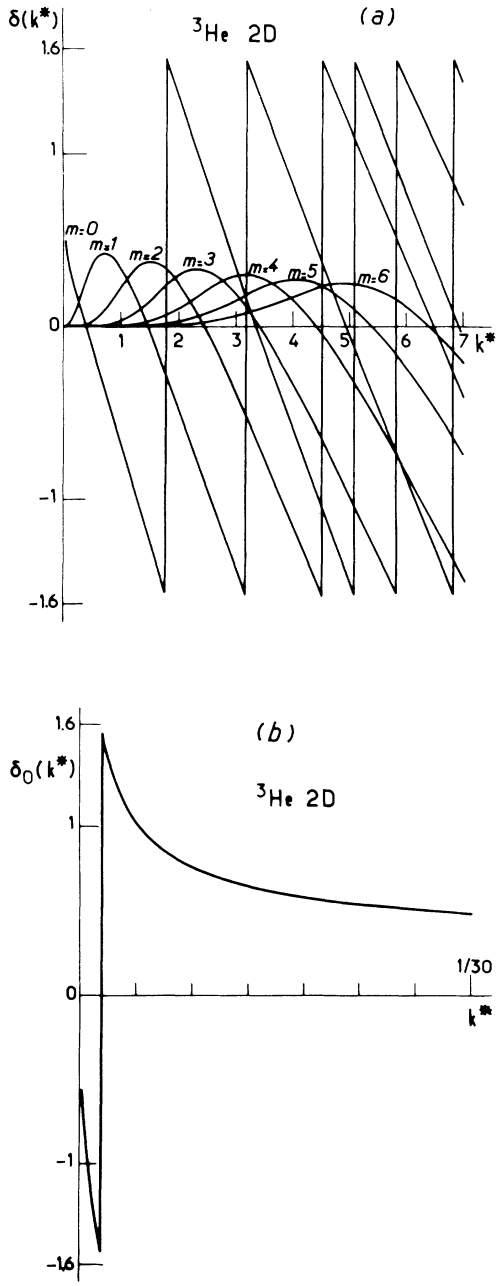

FIG. 9(a) 2D scattering phase shifts for ^{3}He calculated from the HFDHE 2 potential of Aziz *et al.* (Ref. 29) as a function of the reduced wave number $k^*=k\sigma$ ($\sigma=2.556$ Å). (b) Very low energy scattering phase shift $\delta_0(k)$ for ^{3}He. Evidence of a loosely bound state occurring at $k_B^*=1.83\times10^{-3}$.

APPENDIX C: 2D BINDING ENERGIES OF ^{3}He$_2$, ^{3}He-^{4}He, ^{4}He$_2$ DIMERS

While it is widely accepted that binding is easier in two dimensions (see Ref. 40 for instance), it has also been stated that a bound state should always be present.[41] These considerations are based on the presence in the reduced Schrödinger equation for $m=0$ quantum number, of a "negative centrifugal barrier" which only appears in 2D,

and which acts as an effective attractive interaction. It can indeed be proved that a bound state always exists in 2D in a potential which is purely attractive[42] whereas in 3D there is a threshold condition in the well depth and range for binding to occur.

The aforementioned work generally assumes a non-singular interatomic potential which excludes the very strong, short-ranged repulsive barrier encountered in realistic systems. Bagchi[43] pointed out numerically the existence of a threshold for binding in 2D as well as an exponential variation of the binding energy versus mass for Lennard-Jones potentials; however his formal demonstration of these features relies upon the assumption of a non-singular potential.

We show formally in Sec. 1 that this assumption can be released and that, in the presence of a hard-core repulsion, there is a threshold condition for binding and an exponential dependence of the binding energy with the coupling constant. Our numerical results are given in Sec. 2.

1. Simple model: Hard-core repulsion plus attractive well

We consider here the interaction potential $V(r)$ already defined in Appendix B Sec. 2 *c*, consisting of a hard-core-repulsive potential of radius σ and a square attractive well of depth $-V_0=-\hbar^2\mathcal{K}_0^2/2\mu$ located between $r=\sigma$ and $r=R\geq\sigma$.

The existence of a bound state in such a potential and its binding energy $E_B=-\hbar^2k_B^2/2\mu$ are determined by the matching of the logarithmic derivatives of the wave function describing this bound state in regions II and III. The equation to be solved is

$$\left.\frac{R\dot{\psi}_{\rm II}(r)}{\psi_{\rm II}(r)}\right|_{r=R}=\left.\frac{Rk_B\dot{K}_0(k_Br)}{K_0(k_Br)}\right|_{r=R}, \tag{C1}$$

where, to the lowest order in $k_B/\mathcal{K}_0$,

$$\psi_{\rm II}(r)=N_0(\mathcal{K}_0\sigma)J_0(\mathcal{K}_0r)-J_0(\mathcal{K}_0\sigma)N_0(\mathcal{K}_0r) \tag{C2}$$

clearly satisfies $\psi_{\rm II}(\sigma)=0$. For $k_BR\ll1$, the right side of (C1), which is always negative, tends towards $(\ln k_BR+C)^{-1}\sim0$, so that the condition for a bound state to exist is

$$\left.\frac{R\dot{\psi}_{\rm II}(r)}{\psi_{\rm II}(r)}\right|_{r=R}\leq0\ . \tag{C3}$$

In loose binding situations, when $\mathcal{K}_0R\ll1$, (C3) then reads

$$\frac{1+(\mathcal{K}_0R)^2/2}{\ln R/\sigma}-\frac{(\mathcal{K}_0R)^2}{2}\leq0 \tag{C4}$$

or equivalently,

$$\frac{R}{\sigma}\geq\exp\left[1+\frac{2}{(\mathcal{K}_0R)^2}\right]. \tag{C5}$$

As stated earlier, this establishes the threshold in the extent of the potential well below which there is no bound state.

If one makes σ tend to zero to suppress the hard-core repulsion, this threshold vanishes to zero. In other words, in two dimensions, even a vanishingly shallow attractive well is able to sustain a bound state, provided that there is no impenetrable region near the origin. This feature has already been mentioned earlier by Landau.[42]

The presence of a hard core repulsion bends the wave function towards the horizontal axis in the region $r\gtrsim\sigma$. This, at the same time, increases the kinetic energy and decreases the potential energy. To compensate these effects and maintain a bound state, it is then necessary to increase the range or depth of the attractive well, or alternatively, the mass of the particle under consideration. This is why a threshold appears.

Just above the threshold, the binding energy is then given by

$$E_B=-\hbar^2k_B^2/2\mu\ ,$$

with

$$\frac{k_BR}{2}=\exp(-C)\exp\left[\frac{\ln(R/\sigma)}{\frac{(\mathcal{K}_0R)^2}{2}\left[\ln\frac{R}{\sigma}-1\right]-1}\right].$$

By comparison, it is easy to establish that, in three dimensions as well as in one dimension, Eq. (C1) is replaced by

TABLE IV. Binding energies of the loosely bound dimers of helium in 2D and 3D for Lennard-Jones and Aziz potentials.

Potential		$^4He_2$	^3He-^4He	$^3He_2$
Lennard-Jones 6-12	3D			
$\varepsilon=-10.22$ K at	2D	-23.6 mK[a]	-1.45 mK[a]	$-4.63.10^{-7}$ K[a]
$r_m=2.87$ Å				
$\sigma=2.556$ Å				
Aziz *et al*, HFDHE2	3D	-0.83 mK[b]		
$\varepsilon=-10.8$ K at	2D	-36.14 mK[c]	-3.38 mK[c]	$-0.88.10^{-5}$ K[c]
$r_m=2.967$ Å				
$\sigma=2.63$ Å				

[a]Reference 24.
[b]Reference 44.
[c]This work.

$$k_B R = -(\mathcal{K}_0 R)\cot[\mathcal{K}_0(R-\sigma)] \ . \quad \text{(C6)}$$

In the presence of a hard-core repulsion, there is also a threshold ($\mathcal{K}_0(R-\sigma) \geq \pi/2$) below which there is no bound state, but, contrary to the two-dimensional case, this threshold still exists in three dimensions when the hard core potential is suppressed. In 1D, the threshold also disappears because the wave function can then be finite at the origin so that (C6) is replaced by $k_B R = \mathcal{K}_0 R \tan(\mathcal{K}_0 R)$.

On the other hand, when $\mathcal{K}_0 R$, $\mathcal{K}_0 \sigma \gg 1$, the two-dimensional condition (C3) meets (C6). Close to the threshold $\mathcal{K}_0(R-\sigma)=\pi/2$, the potential looks like a narrow well close to a large impenetrable barrier; the 2D "negative centrifugal barrier" then has little effect, so that accomodate a bound state in 2D is not easier than in 1 or 3D.

Nevertheless when (C3) and (C6) are compared, it can also be shown that, more generally, for any value of $\mathcal{K}_0 R$, a bound state always appears for lower values of R/σ in 2D than in 1 or 3D, which means that in such a potential as given by (B5), binding is always easier in 2D. This statement can be extended to Lennard-Jones-type potentials since, in essence, the specificity of 2D has its origin in the "negative centrifugal barrier" appearing in the reduced Schrödinger equation.

2. Binding energy of ^{3}He in two dimensions

The ground-state binding energy $E_B = -\hbar^2 k_B^2/2\mu$ is found by solving the radial Schrödinger equation written in its reduced form as in (B3) for $m=0$

$$-\ddot{v}_0 + \left[U - \frac{1}{4r^2} + k_B^2\right] v_0 = 0 \ .$$

The presence of the "negative centrifugal barrier" introduces an effective potential with slightly modified core radius and well depth. In the region $r \simeq \sigma$, the order of magnitude of $\hbar^2/8\mu r^2$ is 0.6 K, only 6% of the well depth $\epsilon = -10.8$ K of the Aziz potential. As a consequence, the effective potential is very close to the bare potential in this region. This "negative barrier" exerts a significant influence at $r = 3\sigma \sim 7.5$ Å where it is equal to the bare potential (~ 60 mK). This of course, is even more pronounced beyond this distance, since the van der Waals attraction $-C_6/r^6$ then decreases more rapidly.

On the overall, these modifications might seem negligible. Nevertheless, it must be recalled that the Lennard-Jones potential used in the past for He with its well depth of $\epsilon = -10.22$ K was not strong enough to allow a bound state for ^{4}He in 3D, whereas the potential proposed by Aziz with $\epsilon = -10.8$ K led to the binding energy given by Stwalley *et al.*[44] (see Table IV). It is then not surprising that a bound state can be found for ^{3}He in 2D.

The computation of the binding energy was done by solving the Schrödinger equation following a Numerov process. Our program was checked to reproduce the binding energy of ^{4}He in 3D computed by Stwalley *et al.*[44] Taking into account the "negative centrifugal barrier" specific to the two dimensional case, we then found the energy of the bound state of two ^{3}He atoms in 2D: $E_B^{2D}(^3\text{He}\text{-}^3\text{He}) = -0.88 \times 10^{-5}$K. [The binding energies presented here were calculated with the 1973 recommended masses $m(^4\text{He}) = 4.002\,603\,267$ (a.u.) and $m(^3\text{He}) = 3.016\,029\,306$ (a.u.). But since the phase shifts were calculated with a less recent ^{3}He mass $= m(^3\text{He}) = 3.015\,30$, we also computed the binding energy with this lower value of the mass and found $E_B = -0.86 \times 10^{-5}$ K. This shows that a 2×10^{-4} change of the mass is able to produce a 2% change of the binding energy.]

This value was carefully checked against possible changes due to the integration step which was 0.05 Å, the integration range covering at most 5000 Å. We also performed the same calculation for ^{3}He-^{4}He and ^{4}He-^{4}He. Our results are shown in Table IV. Compared to each other, these binding energies show a striking sensitivity towards changes of the mass.

Their sensitivity toward small change in the potential is equally large, as illustrated in Table IV by the results obtained with the Lennard-Jones potential by Siddon and Schick.[24] This extreme sensitivity toward the mass and small variations of the interaction was clearly announced by the simple model of Sec. 1. It explains why any attempt to design a scaling procedure is doomed to failure in the case of light quantum gases.

[1]For a general review, see the abstracts of the 1979 Aussris Conference on Spin Polarized Quantum Systems [J. Phys. Colloq. **41**, C7 (1980)] and references therein.

[2]V. P. Silin, Zh. Eksp. Teor. Fiz. **33**, 495 (1957); **33**, 1227 (1957) [Sov. Phys.—JETP **6**, 387 (1958); **6**, 945 (1958)].

[3]A. J. Leggett, J. Phys. C **3**, 448 (1970); A. J. Leggett and M. J. Rice, Phys. Rev. Lett. **20**, 586 (1968).

[4]E. P. Bashkin and A. Meyerovich, Pis'ma Zh. Eksp. Teor. Fiz. **26**, 696 (1977) [Sov. Phys.—JETP Lett. **26**, 534 (1977)]; Adv. Phys. **130**, 1 (1981); Usp. Fiz. Nauk **30**, 279 (1980) [Sov. Phys.—Usp. **23**, 156 (1980)]; A. Meyerovich, Phys. Lett. **A69**, 279 (1978); J. Low Temp. Phys. **47**, 271 (1982).

[5]W. J. Mullin and K. Miyake, J. Low Temp. Phys. **53**, 313 (1983).

[6]A. Dutta and C. N. Archie, Phys. Rev. Lett. **55**, 2949 (1985).

[7]G. Bonfait, L. Puech, A. S. Greenberg, G. Eska, B. Castaing, and D. Thoulouze, Phys. Rev. Lett. **53**, 1092 (1984); G. Bonfait, L. Puech, B. Castaing, D. Thoulouze, Europhys. Lett. **1**, 521 (1986).

[8]D. Vollhardt, Rev. Mod. Phys. **56**, 99 (1984).

[9]K. S. Bedell and C. Sanchez-Castro, Phys. Rev. Lett. **57**, 854 (1986).

[10]E. P. Bashkin, Pis'ma Zh. Eksp. Teor. Fiz. 33 **11**, (1981) [Sov. Phys.—JETP Lett. **33**, 8 (1981)].

[11]C. Lhuillier and F. Laloë, J. Phys. (Paris) **40**, 239 (1979); **43**, 197 (1982); **43**, 225 (1982); C. Lhuillier, *ibid.*, **44**, 1 (1983).

[12]B. R. Johnson, J. S. Denker, N. Bigelow, L. P. Levy, J. H. Freed, and D. M. Lee, Phys. Rev. Lett. **52**, 1508 (1984).

[13]B. R. Johnson, Ph.D. thesis, Cornell University, 1984.

[14]W. J. Gully, and W. J. Mullin, Phys. Rev. Lett. **52**, 1810

(1984).

[15]P. J. Nacher, G. Tastevin, M. Leduc, S. B. Crampton, and F. Laloë, J. Phys. (Paris) Lett. **45**, L441 (1984); G. Tastevin, P. J. Nacher, M. Leduc, and F. Laloë, *ibid.* **46**, L249 (1985).

[16]E. P. Bashkin, Pis'ma Zh. Eksp. Teor. Fiz. **40**, 383 (1984) [Sov. Phys.—JETP Lett. **40**, 1197 (1984)].

[17]J. M. V. A. Koelman, H. J. M. F. Noteborn, L. P. H. DeGoey, B. J. Verhaar, and J. T. M. Walraven, Phys. Rev. B **32**, 7195 (1985).

[18]R. Barbé F. Laloë, and J. Brossel, Phys. Rev. Lett. **34**, 1488 (1975); V. Lefevre-Sequin, P. J. Nacher, J. Brossel, W. N. Hardy, and F. Laloë, J. Phys. **46**, 1145 (1985).

[19]R. Chapman and M. Bloom, Can. J. Phys. **54**, 861 (1976).

[20]S. B. Crampton, J. J. Krupczak, and S. P. Souza, Phys. Rev. A **25**, 4383 (1982).

[21]L. Pierre, H. Guignes, and C. Lhuillier, J. Chem. Phys. **82**, 496 (1985).

[22]I. B. Mantz and D. O. Edwards, Phys. Rev. B **20**, 4518 (1979).

[23]Yu Kagan, G. V. Shlyapnikov, I. A. Wartan'yants, and N. A. Glukhov, Pis'ma Zh. Eksp. Teor. Fiz. **35**, 386 (1982) [Sov. Phys.—JETP Lett. **35**, 477 (1982)].

[24]R. L. Siddon and M. Schick, Phys. Rev. A **9**, 907 (1974).

[25]E. V. L. Mello, J. J. Rehr, and O. E. Vilches, Phys. Rev. B **28**, 3759 (1983). Formula (A2) does not specify the weights of the different phase shifts. More explicitly, the last term in (A2) should read

$$-\frac{2^{3/2}\lambda^5}{\pi^2}\int_0^\infty dk\,k\sum_l{}'(2l+1)\delta l(k)\,l^{-\beta E(k)},\quad \text{in 3D},$$

$$-\frac{2\lambda^4}{\pi^2}\int_0^\infty dk\,k\sum_{m=-\infty}^{+\infty}{}'\delta_m(k)\,e^{-\beta E(k)},\quad \text{in 2D}.$$

An incorrect weighting might explain the wrong sign and too large difference $[B_{2_{\text{single}}}(M=1)-B_{2_{\text{mixture}}}(M=0)]$ given by these authors, in 3D as well as in 2D, from about a few Kelvins and above.

[26]K. Huang, *Statistical Mechanics* (Wiley, New York, 1963), Chap. 14, Secs. 2 and 3.

[27]V. Lefevre-Seguin, P. J. Nacher, C. Lhuillier, and F. Laloë, J. Phys. (Paris) **43**, 1199 (1982).

[28]P. de Smedt and G. Stragier, J. Phys. A **15**, 2483 (1982).

[29]R. A. Aziz, V. P. S. Nain, J. S. Carley, W. L. Taylor, and G. T. McConville, J. Chem. Phys. **70**, 4330 (1979).

[30]L. P. Levy and A. E. Ruckenstein, Phys. Rev. Lett. **52**, 1512 (1984).

[31]C. Lhuillier and F. Laloë, Phys. Rev. Lett. **54**, 1207 (1985).

[32]B. J. Verhaar, L. P. H. de Goey, J. P. H. W. Van den Eignde, and E. J. D. Vredenbregt, Phys. Rev. A **32**, 1424 (1985).

[33]E. Merzbacher, *Quantum Mechanics* (Wiley, New York, 1963).

[34]I. Richard Lapidus, Am. J. Phys. **50**, 45 (1982).

[35]S. K. Adhikari, Am. J. Phys. **54**, 362 (1986).

[36]D. Bollé and F. Gesztesy, Phys. Rev. Lett **52**, 1469 (1984).

[37]B. J. Verhaar, J. P. H. W. Van den Eigjnde, M. A. J. Voermans, and M. M. J. Schaffrath, J. Phys. A **17**, 595 (1984).

[38]N. Kolos and L. Wolniewicz, Chem. Phys. Lett. **24**, 457 (1974).

[39]I. F. Silvera, Rev. Mod. Phys. **52**, 393 (1980).

[40]M. Papoular, J. Phys. B **18**, L821 (1985).

[41]E. P. Bashkin, Zh. Eksp. Teor. Fiz. **78**, 360 (1981) [Sov. Phys.—JETP **51**, 181 (1980)].

[42]L. D. Landau and E. M. Lifshitz, *Quantum Mechanics* (Pergamon, London, 1958), Chap. VI, Sec. 45, and related problems.

[43]A. Bagchi, Phys. Rev. A **3**, 1133 (1971).

[44]Y. H. Uang and W. C. Stwalley, J. Chem. Phys. **76**, 5069 (1982).